UNIVERSITY OF BIRMINGHAM
University of Birmingham

Electrochemical Impedance Spectroscopy of Li-S Batteries

Fazal, Hira; Eroglu, Damla; Kilic, Aysegul; Ali, Nazakat; Yan, Changyu; Zai, Jiantao; Qian, Xuefeng

Document Version
Publisher's PDF, also known as Version of record

Citation for published version (Harvard):
Fazal, H, Eroglu, D, Kilic, A, Ali, N, Yan, C, Zai, J & Qian, X 2024, 'Electrochemical Impedance Spectroscopy of Li-S Batteries: Effect of Atomic Vanadium- and Cobalt-Modified Ketjen Black-Sulfur Cathode, Sulfur Loading, and Electrolyte-to-Sulfur Ratio', *ChemElectroChem*. https://doi.org/10.1002/celc.202300781

Link to publication on Research at Birmingham portal

ChemElectroChem

Research Article
doi.org/10.1002/celc.202300781

Chemistry Europe
European Chemical Societies Publishing

www.chemelectrochem.org

Electrochemical Impedance Spectroscopy of Li-S Batteries: Effect of Atomic Vanadium- and Cobalt-Modified Ketjen Black-Sulfur Cathode, Sulfur Loading, and Electrolyte-to-Sulfur Ratio

Hira Fazal,[a, b, c] Damla Eroglu,*[a] Aysegul Kilic,[a] Nazakat Ali,[b, d] Changyu Yan,[b] Jiantao Zai,[b] and Xuefeng Qian*[b]

The polysulfide shuttle mechanism and insulating characteristics of sulfur and discharge products are the two major drawbacks of Li–S batteries. These increase internal cell resistances, resulting in low battery performance and life. In this study, we investigate the effect of cathode material on the cell resistances by preparing two different cathodes: by encapsulating sulfur (S) with pure Ketjen black (KBS) and with atomic vanadium and cobalt-modified Ketjen black (VCKBS). In addition to the cathode material, the influence of crucial cell design parameters, namely electrolyte-to-sulfur (E/S) ratio and sulfur loading, on the cell resistances and battery performance is also compared. Electrochemical impedance spectroscopy (EIS) is applied to determine the individual cell resistances, whereas a system-level performance model is used to estimate the system-level specific energies and energy densities. The comparison of the cathodes shows that VCKBS significantly improves both cell- and system-level performances, which are attributed to a significant decrease in cell resistances. The cells with higher sulfur loadings and lower E/S ratios show poorer performance for both cathodes. On the other hand, an E/S ratio of 6 mg L^{-1} can result in high cell- and system-level performances for the VCKBS cathode.

Introduction

Lithium-sulfur (Li–S) batteries have emerged as a 'hot topic' in both battery research and industry due to their potential low cost and eco-friendliness, coupled with a noteworthy theoretical energy density of 2600 Wh/kg for S cathodes, which is six times that of Li-ion batteries utilizing $LiCoO_2$ and graphite electrodes.[1,2] Despite their potential advantages, the practical employment of Li–S batteries is still hampered by various challenges concerning poor energy utilization and efficiency. Current approaches to solve the challenges of the sulfur cathodes generally involve synthesizing new materials for trapping sulfur and enhancing electronic conductivity; typically, these materials are carbon-based[3,4] and are utilized in surface coating, encapsulation, and impregnation procedures. These strategies aim to improve the electronic conductivity of S cathodes while preventing the dissolution of polysulfide species.[5,6]

In addition to functional materials development, a proper cell design is also critical, especially for the system-level efficiency of the Li–S batteries, where all the cell components are included in the gravimetric and volumetric energy density calculations. Hence, cell design and material development should be studied simultaneously. The Li–S battery performance is heavily dependent on cell design parameters; most importantly, the battery performance becomes quite different by varying sulfur loadings and electrolyte-to-sulfur (E/S) ratios. Low S loadings and high E/S ratios are typically used to increase specific capacity and cycle life, though these cells will end up with low system-level performances.[7,8,9] Cells' dead mass, including electrolytes, should be minimized for practical applications with maximized active material loadings.[10,11] If a high sulfur loading is not attained in an actual electrical device, the practical energy density of the battery will be considerably hampered.[12,13] Therefore, a thorough investigation of the impact of sulfur loading per unit area on the effectiveness of Li–S batteries is crucial. In Li–S cells, the intermediate product is soluble, resulting in a direct correlation between the electrolyte content and the amount of the dissolved polysulfides, as well as subsequent nucleation and re-deposition processes. Therefore,

[a] Dr. H. Fazal, Prof. Dr. D. Eroglu, A. Kilic
Department of Chemical Engineering
Bogazici University
Istanbul, 34342, Turkey
E-mail: eroglud@boun.edu.tr

[b] Dr. H. Fazal, Dr. N. Ali, C. Yan, Prof. Dr. J. Zai, Prof. Dr. X. Qian
Department of Chemistry and Chemical Engineering
Shanghai Jiao Tong University
Shanghai, 200240, P.R. China
E-mail: xfqian@sjtu.edu.cn

[c] Dr. H. Fazal
Present Address: School of Metallurgy and Materials
University of Birmingham
Birmingham, B15 2TT, UK

[d] Dr. N. Ali
Present Address: Department of Chemistry
University of Oxford
Oxford, OX1 3QR, UK

ChemElectroChem

Research Article
doi.org/10.1002/celc.202300781

Chemistry Europe
European Chemical
Societies Publishing

the electrolyte's function in Li–S batteries is more complicated than anticipated, and further comprehensive investigations are necessary to determine the optimal electrolyte amount that can enhance both cell- and system-level performances.[14,15]

For characterizing the kinetic and transport mechanisms in electrochemical systems, notably in batteries, the use of electrochemical impedance spectroscopy (EIS) is very common.[16,17] A battery's internal resistance is an important feature that significantly impacts its operating voltage, rate capability, and practical capacity. In the reported literature, various studies characterized Li–S batteries utilizing the EIS technique, measuring cell resistances at a particular cycle number or depth of discharge (DoD).[15,18,19,20] These reports mainly examine the influence of cathode and electrolyte components on cell resistance.[21,22] Yet, research on the critical relationship involving cathode design and the complex mechanisms for different materials in Li–S cells is inadequate. Using a revised intermittent current interruption methodology, Lacey investigated the impact of the E/S ratio on Li–S cell resistance.[23] The EIS approach was used by Sun et al. to investigate the effect of S loading on cathode mechanisms.[24] Previously, our group also reported the effect of carbon-to-sulfur (C/S) and E/S ratios on Li–S battery resistance using EIS.[25] All these results prove that cell structure has a key role in its resistance. Although the EIS method has been extensively utilized to study Li–S batteries, a more comprehensive investigation is necessary to characterize the influence of crucial cathode specifications on cell resistance, especially for novel encapsulated sulfur cathodes. The previous literature typically focuses on the interpretation of experimental EIS results, yet here, we provide experimental findings along with system-level performance predictions. We not only compare the behavior of two different materials, a commercial material, and a specifically designed novel composite, but we also report the impact of the E/S ratio, S loading, and material characteristics on the cell- and system-level performances of the Li–S batteries.

In a recent study, we described a straightforward, viable, and cheap method for producing an atomic vanadium (V) and cobalt (Co) modified Ketjen black (KB)-sulfur composite (VCKBS) as a cathode host for Li–S batteries.[26] When compared to the sulfur cathode encapsulated with pure Ketjen black, Li–S cells with the VCKBS cathodes showed significantly improved performance due to the presence of abundant interfacial active sites; the addition of Co provided catalytic activity, whereas V offered polysulfide adsorption capability.[26] Therefore, to better understand the limits of the proposed material, the impact of prepared cathodes on the cell resistance and, hence, the Li–S battery performance is mechanistically studied here. Moreover, the impact of S loading and E/S ratio on the cell resistance of both cathode materials (VCKBS and KBS) is analyzed via the EIS technique. Finally, an experimentally driven system-level performance model is offered to forecast the impact of these crucial factors on the energy density of the battery. We are confident that our results demonstrate the connection between cathode materials characteristics and cell design parameters to the complex processes occurring in the cells and permit us to understand their effect on the cell resistance, discharge capacity, cycle life, and eventually system-level performance of Li–S batteries.

Results and Discussion

In our previously reported work, the synthesis of the materials was confirmed by various characterization methods.[26] The SEM images and EDX mapping of the materials are provided in Figure S1. To investigate the effect of the S loading and the E/S ratio on the cell resistances, Li–S cells were fabricated with E/S ratios of 6, 13, 20, 35 mL g^{-1} and S loadings of 0.8, 1.2, and 3 mg cm^{-2} using KBS and VCKBS composites as cathode materials. We haven't reported results for Li–S cells with the VCKBS cathode at 35 mL g^{-1} since this E/S ratio is too high for a specifically designed composite cathode. On the other hand, such high E/S ratios are still relevant for more traditionally prepared cathodes such as KBS. The cells were discharged at a 0.1 C rate, and the discharge profiles obtained for the cells with S loading of 1.2 mg cm^{-2} and E/S ratio of 20 mL g^{-1} for KBS and VCKBS cathodes are presented in Figure 1a and Figure 1d, respectively. The impedance spectra of the cells are taken before the first discharge (after rest for 16 hours) and after the 1st, 10th, and 20th discharge (Figure 1b and Figure 1e). The first 20 cycles are typically when significant capacity losses occur, and the cycling performance of the cells is relatively similar after that point. Thus, the general trends of how resistances vary with cycling can be understood this way. It is evident from the figures that cycling has a significant impact on the impedance spectra of the Li–S cell as the semicircles grow larger with cycling, indicating an increase in resistances. To determine the resistance values numerically and compare the results quantitatively, all the EIS spectra are fitted to an equivalent circuit. Representative fitting results for the EIS spectra after the 20th discharge are illustrated in Figure 1c and Figure 1f, with the proposed equivalent circuit visible in the insets. The figure shows that the suggested equivalent circuit accurately captures the experimental results, with a fitting error of $\chi^2/|Z| < 0.1$. It is worth noting that several equivalent circuits can fit the same data; however, simpler circuits with physical meanings of individual elements that can be assigned should be preferred. The obtained spectra contain semicircles in the middle-frequency region and linear lines at the low frequency, as demonstrated in Figure S1-S4. In an EIS spectrum, a semicircle represents a resistance (R) element connected to a capacitor in parallel, a constant phase element (CPE) if the capacitance is not ideal, and the low-frequency lines can be represented by the Warburg impedance element (W).[27] The equivalent circuit used in this study includes two resistances (R_1 and R_2) coupled by one CPE (Q_2) and one W (W_2) circuit element. In the literature, R_e (~R_1) is commonly attributed to electrolyte resistance. At the same time, R_{ct} (~R_2) is ascribed as charge-transfer resistance in the cathode, which is seen in the mid-to-low-frequency area, designated as the kinetically controlled part of the Nyquist plot, at the second extrapolated intersection with the real axis.[28] The CPE, represented by Q_2, is connected to the solid-state diffusion of Li$^+$ as a result of the

ChemElectroChem

Research Article
doi.org/10.1002/celc.202300781

Chemistry
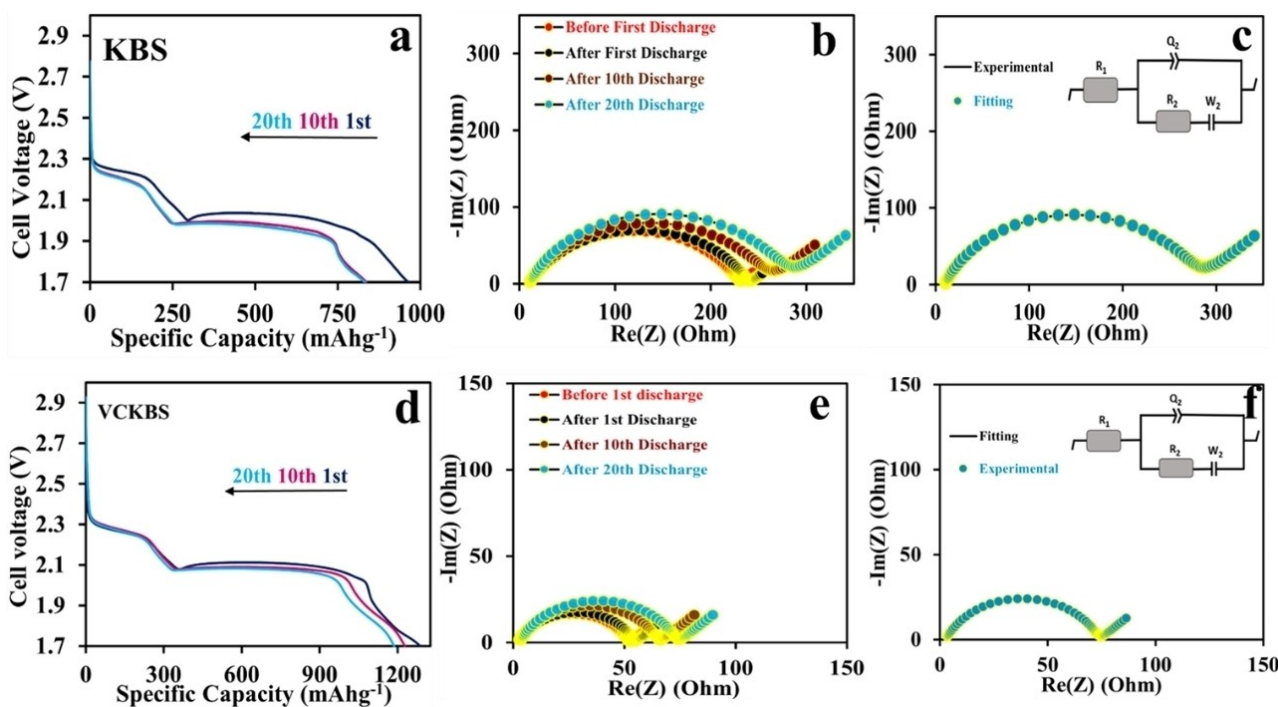Europe
European Chemical
Societies Publishing

Figure 1. KBS composite cathode: a) The 1st, 10th, and 20th discharge profiles, b) EIS spectra at the end of various discharges, c) experimental EIS data and the corresponding fit of the spectrum for a Li–S cell with E/S ratio $=20$ mL g^{-1} and S loading $=1.2$ mg cm^{-2} after the 20th discharge. VCKBS composite cathode: d) The 1st, 10th, and 20th discharge profiles, e) EIS spectra at the end of various discharges, f) experimental EIS data and the corresponding fit of the spectrum for a Li–S cell with E/S $=20$ mL g^{-1} and S loading $=1.2$ mg cm^{-2} after the 20th discharge. Insets show the proposed equivalent circuit for the cells.

formation of a double-layer capacitor between the electrolyte and cathode interface. W_2 represents the Warburg impedance element attributed to the diffusion of Li$^+$ in active materials.[27] Here, all resistances are assumed to be intimately related to the cathode. Previous literature discusses that Li–S cell resistance is commonly dominated by the cathode.[20] However, resistances associated with the SEI formation on the anode may be apparent in the high-frequency region, changing significantly during the first few cycles.[29] As seen in Figure 1b and 1e, there is no particular change in the high-frequency region of the impedance spectra for the cells before and after the 1st discharge, indicating that the contribution of the anode resistances is minor. Consequently, we can relate the changes in the resistances to the transformations in the cathode.[25]

Impact of E/S Ratio on Li-S Cell Resistance for KBS and VCKBS Cathodes

The impact of the E/S ratio on cell resistances is explored by evaluating the EIS results of Li–S cells having E/S ratios of 6, 13, 20, and 35 mL g^{-1} with an S loading of 1.2 mg cm^{-2} for KBS cathodes. Qualitative analysis can be done by comparing the spectra of the cells with different parameters. Figure S2 can be seen as an example to observe qualitatively how the resistance values change with respect to the E/S ratio and cycling; both have a noteworthy impact on the resistances in Li–S cells. Figure S2a shows the impedance spectra for all cells after rest for 16 hours, having different E/S ratios. In the low-frequency

region, the EIS spectra of the cells present an oblique straight line corresponding to the Li$^+$ diffusion process. In the medium-frequency region, a semicircle relevant to the charge transfer resistance is observed. The largest semicircle is found for the cell with an E/S ratio of 6 mL g^{-1}; it continuously contracts with increasing E/S ratio up to 20 mL g^{-1}, while E/S ratio $=35$ and 20 mL g^{-1} depicts related spectra. Figure S2b presents impedance after the first discharge; the semicircles get bigger for all E/S ratios, exhibiting that the charge transfer resistance increases the most in this case. A further increase in the size of the semicircles after the 10th and 20th discharge (Figure S2c and S1d) suggests an increase in the charge transfer resistance with cycling. We can also see the Warburg elements in the spectra. According to previous studies, the Warburg resistance results from polysulfide diffusion into the electrolyte in the liquid state or into the bulk of the cathode in the solid state.[28] A noticeable impact is also found regarding the Warburg resistance in the cathode, and relevant constants are given in Table S1. Similar qualitative discussions can also be made for VCKBS cathodes (Figure S3).

All EIS results have been fitted to the equivalent circuit to obtain quantitative results. Figure 2a and 2d show the influence of the E/S ratio on the electrolyte resistance as a function of the cycle number for KBS and VCKBS cathodes, respectively. A general tendency for the change of electrolyte resistance with discharge number is noticed for both cathodes: electrolyte resistance increases as discharge number increases. The polysulfides (i.e., Li$_2$S$_8$, Li$_2$S$_6$) that develop and dissolve during cycling raise the electrolyte's resistance by altering its viscosity.

ChemElectroChem

Research Article
doi.org/10.1002/celc.202300781

Chemistry Europe
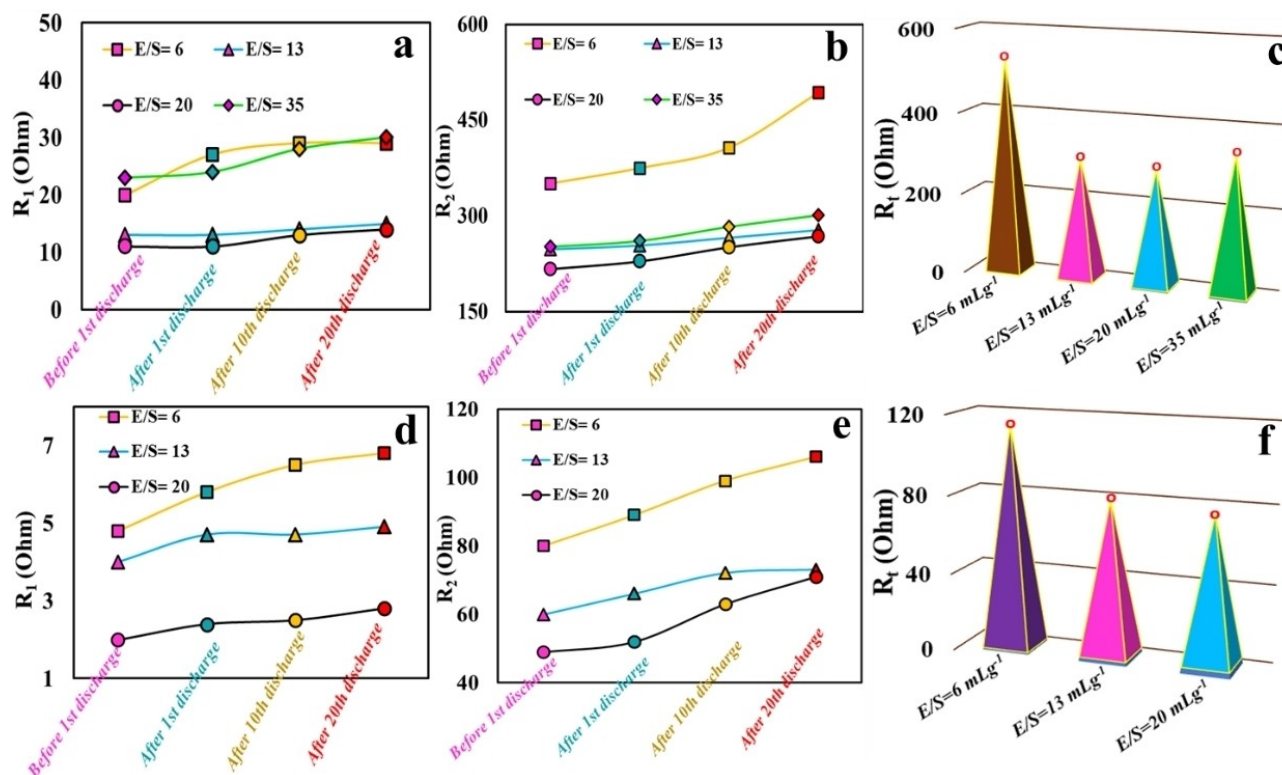European Chemical
Societies Publishing

Figure 2. The effect of the E/S ratio on the a) and d) electrolyte and b) and e) charge transfer resistances as a function of the number of discharge, and c) and f) total cell resistances for the Li–S cells after the 20th discharge at 0.1 C for Li–S cells with KBS and VCKBS cathodes, respectively. S loading = 1.2 mg cm^{-2} for all cells.

The effect of the electrolyte quantity on the resistance is also apparent in the figure. Lower E/S ratios are shown to result in higher electrolyte resistances. This can also be explained by the increased polysulfide concentrations at these low E/S ratios, which result in the electrolyte's increased viscosity and subsequently decreased Li$^+$ conductivity.[30] As seen in the figure, increasing the electrolyte content to E/S = 20 mL g^{-1} lowers resistance throughout all cycles. Interestingly, electrolyte resistances increase at the highest E/S ratio of 35 mL g^{-1}.[15,25] As known, the electrolyte resistance is closely linked to the type and concentration of the dissolved polysulfides, and the polysulfide shuttle mechanism is enhanced at high E/S ratios since polysulfide dissolution is much higher. This may be the reason for the rise in the resistance at the highest E/S ratio.

Figure 2b and 2e confirm that the charge transfer resistance is also highly dependent upon the E/S ratio in the Li–S cell, with the lowest charge transfer resistance achieved for cells with an E/S ratio of 20 mL g^{-1} and the greatest with an E/S ratio of 6 mL g^{-1}. The charge transfer resistance substantially drops when the E/S ratio rises. Li$^+$ ion transport to the cathode active surface may be hampered by electrolyte deficiency. Moreover, at low E/S ratios, the restricted solubility of polysulfides in the electrolyte could prevent electrochemical reactions from occurring. With a lower E/S ratio, these factors increase charge transfer resistance, while an increased electrolyte amount in the cell improves polysulfide dissolution and, as a result, cathode kinetics. Yet, with an excessive amount of electrolyte (E/S =

35 mL g^{-1}), the easy migration of dissolved polysulfides to the lithium metal anode can result in a decrease in the active material amount, leading to an increase in the charge transfer resistance.[15,31] This suggests that the E/S ratio significantly affects reaction kinetics.

In addition, the resistance values constantly increase with cycling, most dominantly for the lowest E/S ratio. This may be due to the inhomogeneous deposition of Li$_2$S, the insulating end-discharge product. Hence, it is harder for the electrochemical reactions to occur due to ionic and electronic conductivity problems at high discharge numbers. This may be one of the reasons why Li–S cells fail at high discharge numbers in electrolyte-starved cells. On the other hand, when the resistance values of the two cathodes are compared, it is seen that the values are much lower for Li–S cells with the VCKBS cathode. As it is stated, the concentration of polysulfides affects electrolyte resistance.[20] Hence, lower electrolyte resistance may indicate the better PS adsorption ability of the VCKBS cathodes. A similar explanation can also be made for the charge-transfer resistances in the cell. Likewise, VCKBS cathodes have much lower charge transfer resistances, which can be attributed to adsorbed PSs on the surface and, thus, better reaction kinetics. This demonstrates once more how effective VCKBS is at reducing polysulfide shuttling and preventing the development of a solid Li$_2$S$_2$/Li$_2$S insulating layer on the electrode surface. Further evidence that the tight contact between S and the modified KB and the uniform dispersal of sulfur in the

composite are advantageous for electrode conductivity and charge transfer inside the electrode may be found in the significantly lower R_{ct} values observed for VCKBS. In parallel to these discussions, it is found that total cell resistance is very reliant on both the E/S ratio and cathode material, as visible in Figure 2c and Figure 2f, and materials with tailored properties can significantly decrease the internal cell resistances, especially in electrolyte-deprived cells.

Impact of S Loading on Li-S Cell Resistance for KBS and VCKBS Cathodes

Similar qualitative analyses can be employed for cells with S loadings of 0.8, 1.2, and 3 mg cm^{-2} and an E/S ratio of 13 mL g^{-1} for both cathode types, using the EIS spectra presented in Figure S4 and S5. Here, it should be mentioned that the S loading of the cells was altered by varying the cathode thicknesses while keeping constant the S wt.% in the cathode, another critical factor influencing the performance. The cell resistances are typically minimized at moderate S wt.% (or carbon-to-sulfur ratios, in other words).[25] Therefore, herein, we choose a moderate S content for identifying the impact of different factors more straightforwardly. To obtain quantitative results, all EIS results have been fitted to the aforementioned equivalent circuit, and Figure 3 provides the replicate cells' average resistances. Figure 3a and 3d show the impact of the S loading on electrolyte resistance as a function of cycle number for KBS and VCKBS cathodes, respectively. In Li–S cells with KBS

cathodes (Figure 3a), cells with S loading = 0.8 mg cm^{-2} show the lowest electrolyte resistance, and the effect of cycling is negligible.

The cells with S loading = 1.2 mg cm^{-2} present comparatively higher electrolyte resistance with a slight dependence on cycling. On the other hand, the electrolyte resistance is significantly higher for S loading = 3.0 mg cm^{-2}, which constantly increases with cycling. At higher sulfur loadings, more sulfur may dissolve in the electrolyte, considerably increasing its viscosity. This can lead to a reduction in the ionic conductivity of the electrolyte, increasing electrolyte resistance. Meanwhile, charge transfer resistance is almost the same for S loadings = 0.8 mg cm^{-2} and 1.2 mg cm^{-2} but significantly higher for 3 mg cm^{-2}, with a prominent increase observed with cycling. When VCKBS cathodes are analyzed (Figure 3d), cells with a moderate S loading (1.2 mg cm^{-2}) show the lowest electrolyte and charge transfer resistances, which differs from KBS cathodes. Li–S cells with an S loading = 0.8 mg cm^{-2} offer higher electrolyte resistance compared to 1.2 mg cm^{-2}; it can be argued that these cells have an inadequate amount of electrolyte, which causes poor cathode wetting and hence Li$^+$ ion transport may be hampered, resulting in an increased electrolyte resistance. Similarly, S loading = 0.8 mg cm^{-2} showed higher charge transfer resistance as compared to higher S loadings. In general, at low sulfur loadings, the active material in the electrode is better distributed and dispersed throughout the electrode, which can lead to a decrease in the charge transfer resistance. However, at low sulfur loadings, the available active material may become too sparse to effectively participate in the
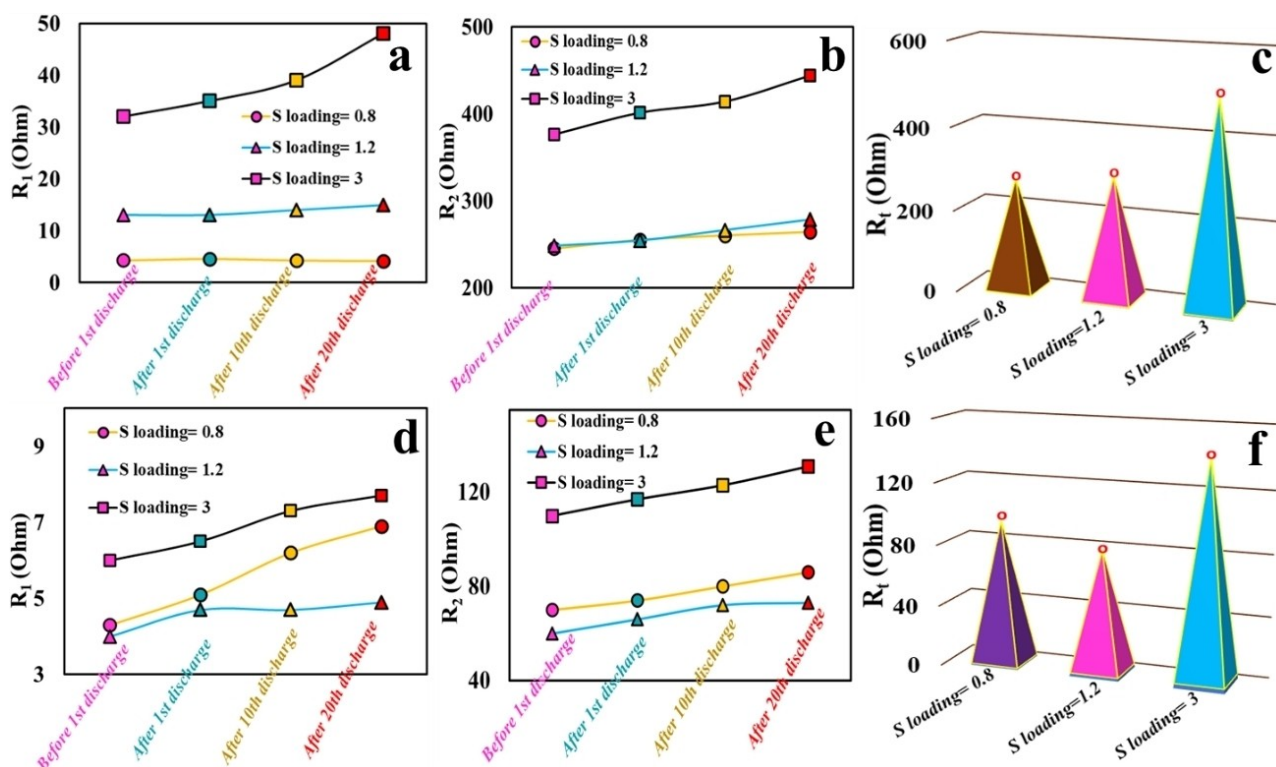

Figure 3. The impact of S loading on the a) & d) electrolyte and b) & e) charge transfer resistances as a function of the number of discharge, and c) & f) total cell resistances for the Li–S cells after the 20th discharge at 0.1 C for Li–S cells with KBS and VCKBS cathodes, respectively. E/S ratio = 13 mL g^{-1} for all cells.

ChemElectroChem

Research Article
doi.org/10.1002/celc.202300781

**Chemistry
Europe**
European Chemical
Societies Publishing

charge transfer reactions and hence affect cathode kinetics negatively, increasing the resistance. It is evident that the S loading has a considerable impact on the resistances in a Li–S cell; particularly, the deficiency or excess of sulfur in the cathode worsens the reaction kinetics. Moreover, it may be discussed that both the number of discharges and S loading profoundly influence the Warburg resistances (Table S1). Because of the accumulation of insoluble discharge products (Li_2S_2/Li_2S), Warburg impedance is apparent in the low-frequency region, specifically for an S loading of 3 mg cm^{-2} after the 20th discharge.

Finally, Figure 3c and 3f show the overall cell resistances as a function of S loading after the 20th discharge. In line with the previous discussions, the Li–S cells exhibit the lowest and the highest overall cell resistances when S loadings of 0.8 mg cm^{-2} and 3 mg cm^{-2} are used for KBS cathodes, respectively, whereas for VCKBS cathodes, the lowest and the highest overall cell resistances are obtained for S loadings of 1.2 mg cm^{-2} and 3 mg cm^{-2}, respectively. Furthermore, when the resistance values are compared between the two cathodes, it is seen that the values are much lower for Li–S cells containing VCKBS cathode, which is due to the combined result of Co and V, causing a higher charge-transfer ability because of their high polysulfide adsorption characteristics and enhanced reaction kinetics. To strengthen our statement, we analyzed the CV results (Figure S6) of the cells with KBS and VCKBS cathodes to study the impact of materials on the electrochemical reaction kinetics. Li–S cells with KBS do not show prominent redox peaks, whereas cells with VCKBS present two discrete peaks at 2.3 and 1.9 V, characteristic of the two-step reduction reactions.

Similarly, two anodic peaks at 2.3 and 2.5 V are apparent in the CV curve of KBS.[32] Consequently, Li–S cells with VCKBS cathodes exhibit superior redox kinetics and enhanced catalytic activity, supporting the reduced total resistance of the Li–S cells with VCKBS cathodes.

Impact of Cell Resistances on the Performance of Li-S Cells with KBS and VCKBS Cathodes

Previous studies[17,33,34] often discuss optimal values for the S loading and the E/S ratio in a battery, maximizing the discharge capacity of the Li–S batteries, which is parallel to our previous findings. To support our results shown here, the cycling efficiency of the cells for both KBS and VCKBS materials (Table S2) having E/S ratios = 6, 13, and 20 mL g^{-1} and S loadings of 0.8, 1.2, and 3 mg cm^{-2} are compared in Figure 4. For both cathodes, E/S ratio = 6 mL g^{-1} and S loading = 3 mg cm^{-2} result in the poorest cell performance, which may be explained by the high internal resistance at lower E/S ratios and higher S loadings in the cell, validating our previous discussion. As the electrolyte resistance increases, the amount of active lithium ions introduced into the pores of the material is limited, and poor reaction kinetics are obtained, declining the cell performance.

Although cell-level specific capacities and cycling performances are essential, system-level specific energy is a more viable performance metric for assessing the commercialization of Li–S batteries.[35,36,37] A modified BatPaC model was used to estimate the system-level performance metrics with the experimentally
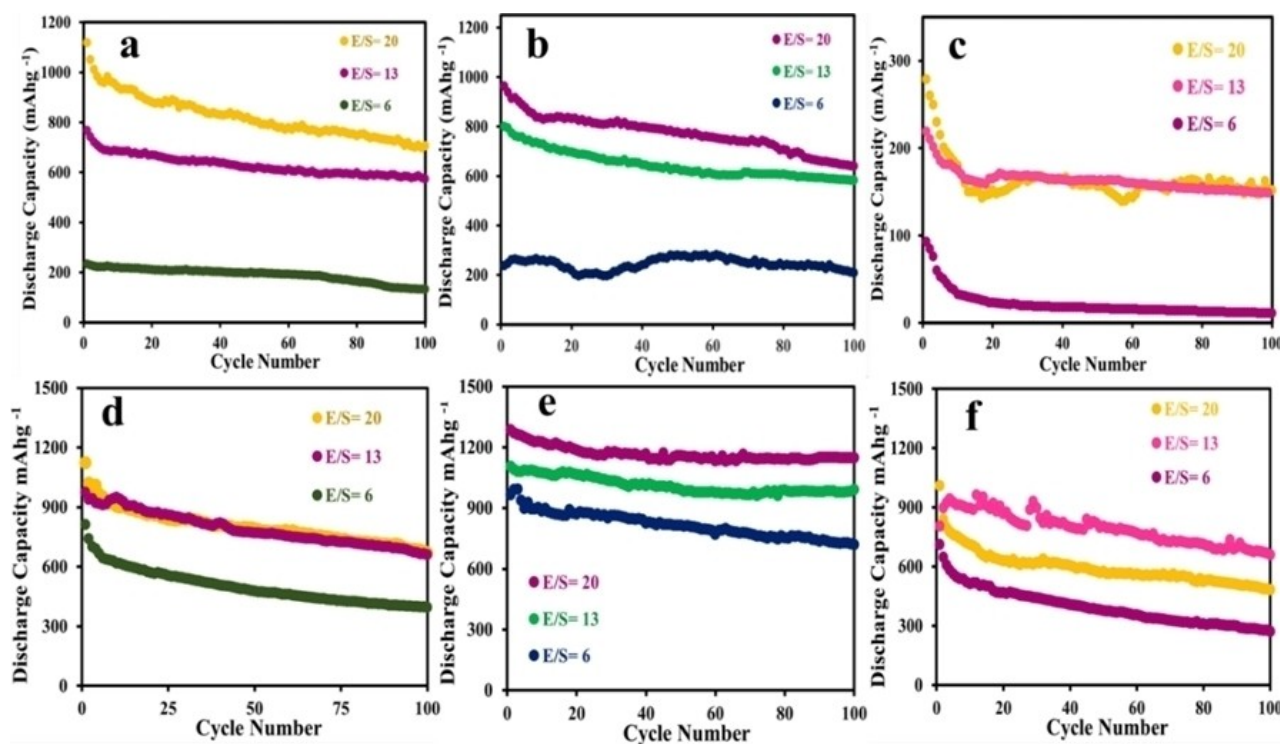

Figure 4. Cycling performances: KBS cathodes with S loadings of (a) 0.8 mg/cm^2, (b) 1.2 mg/cm^2, and (c) 3 mg/cm^2, and VCKBS cathodes with S loadings of (d) 0.8 mg/cm^2, (e) 1.2 mg/cm^2, and (f) 3 mg/cm^2 at 0.1 C.

ChemElectroChem

Research Article
doi.org/10.1002/celc.202300781

**Chemistry
Europe**

European Chemical
Societies Publishing

obtained specific capacities, S loadings, and E/S ratios. Figure 5a shows a decreasing trend in specific capacity for lower E/S ratios and higher S loadings for KBS cathodes. In contrast, maximum capacity is obtained with an S loading $= 1.2$ mg cm^{-2} for VCKBS cathodes. These trends are explained by the change in the cell resistances in the previous subsection. In contrast, corresponding system-level specific energies of Li–S cells containing VCKBS cathodes show an opposite trend to the specific capacity. Lowering the E/S ratio drastically increases the specific energies, with the highest specific energy obtained with a moderate S loading. In contrast, in Li–S batteries with KBS cathodes, the decrease in the specific capacity with decreasing E/S ratio and increasing S loading is too high, and the reduction in the cells' dead mass does not compensate for obtaining higher specific energies. Finally, Figure 5c summarizes the superiority of the VCKBS cathodes over KBS ones, presenting the significantly lower cell resistances and higher specific energies obtained for these novel cathodes, especially at low E/S ratios. To sum up, tailoring cathode properties is critical for lower cell resistances and improved battery performance. The co-dope of Co and V elements boosts the catalytic ability of Co and the absorption ability of V simultaneously. The effect strengthens the intrinsic ability of the active sites. Thus, active sites in the modified KB can accommodate higher S loadings in the cathode. Moreover, since cathode kinetics for the PS transfer are enhanced, lower E/S ratios and higher S loadings can be tolerated.

Conclusions

In conclusion, the E/S ratio, S loading, and cathode material characteristics significantly affect the electrolyte and charge-transfer resistances in a Li–S cell, consequently influencing cell- and system-level performances. This study investigates the effect of cathode material characteristics on the reaction and transport mechanisms by comparing the resistances measured by the EIS method for two cathodes, VCKBS and KBS. Moreover, the influence of the E/S ratio and S loading on these mechanisms is explored for these two cathodes. Lowering the E/S ratio or increasing the loading of S in the cathode both

result in a rise in cell resistance, especially by increasing cycle numbers, which explains the poorer cycling performance seen for these cells. Much lower charge transfer, electrolyte, and total cell resistances are found for Li–S batteries containing VCKBS cathode, which is due to the combined impact of Cobalt and Vanadium, producing a higher charge-transfer efficiency because of their high polysulfide adsorption characteristics and enhanced reaction kinetics. VCKBS cathodes can significantly decrease internal cell resistances, especially at higher S loadings in electrolyte-deprived cells. The lowest cell resistance of Li–S cells having KBS composite is obtained for E/S $= 20$ mL g^{-1} with S loading $= 0.8$ mg cm^{-2}, whereas for VCKBS, sulfur loading of 1.2 mg cm^{-2} showed the minimum resistance. Although lower cell resistances lead to better specific capacities and cycling performance, identifying the dependence of the specific energies at the pack level on the cell resistance is not trivial; VCBKS cathodes with lower E/S ratios excel at specific energies. To conclude, this paper provides mechanistic details for the trends on the impact of the E/S ratio, S loading, and material characteristics on the cell- and system-level performances of the Li–S batteries.

Experimental Section

Synthesis of KBS and VCKBS electrode materials

The experimental procedure involved using analytically pure chemicals without additional treatment. The preparation of VCKBS included a specific weight ratio of Cobalt salt (Co(NO$_3$)$_2$.6H$_2$O) to Ketjen Black (KB) of 1:1.5. Initially, a mixture of 120 mL distilled H$_2$O and 30 mL anhydrous ethanol were combined with the wanted quantity of KB. Subsequently, the resultant mixture was subjected to sonication for 30 minutes. Additionally, deionized (DI) water (20 mL) was utilized to dissolve the Co(NO$_3$)$_2$.6H$_2$O completely, gradually added to the prepared suspension of KB, followed by sonication for two hours. This procedure made it easier for Co^{2+} ions to enter the micro- and mesopores of KB, which encouraged the development of dispersed cobalt nanoparticles. After that, the resulting product was subsequently dried at 60 °C in an oven for a day. To produce the nanostructured Co/KB (CKB), the dried precursor was then subjected to reduction at a temperature of 850 °C (two hours) in an inert environment within a quartz tube. Next, 1.23×10^{-4} moles of V$_2$O$_5$ were dissolved thoroughly by stirring in deionized (DI) water (40 mL) for five hours. Subsequently,
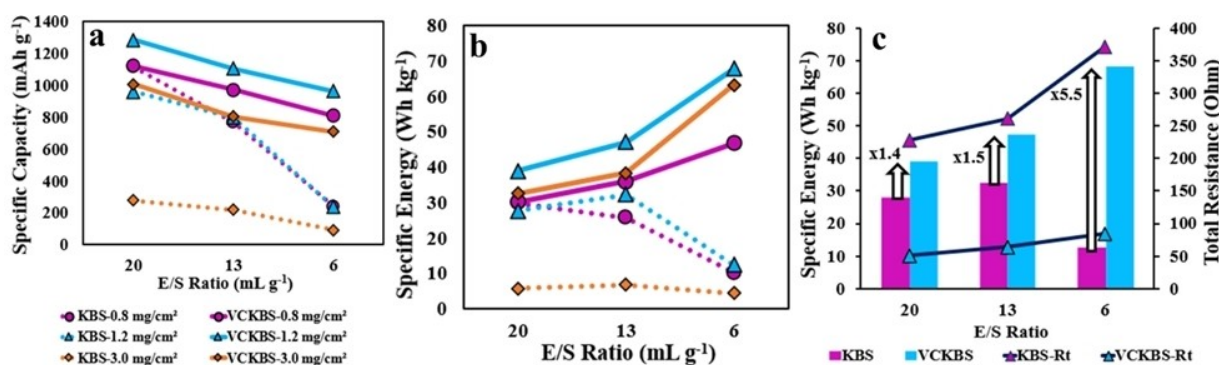

Figure 5. (a) Experimentally measured initial discharge capacities, (b) predicted system-level specific energies for various sulfur loadings and E/S ratios, and (c) the relation between cell resistance and specific energies for sulfur loading $= 1.2$ mg cm^{-2}.

ChemElectroChem

Research Article
doi.org/10.1002/celc.202300781

Chemistry
Europe
European Chemical
Societies Publishing

200 mg of CKB was poured into the aforementioned solution and subjected to sonication for two hours. After centrifugation, the prepared nanocomposite was dried at 60 °C in an oven. In the subsequent step, sulfur was combined with the prepared nanocomposite using a weight ratio of 1 : 1. The mixture was then ground for a period of 8–10 minutes. In order to ensure that sulfur would diffuse into the composite, the resultant powder was then heated in a vacuum oven at 155 °C for 12 hours. This resulted in the formation of VCKBS. A similar procedure was followed for the preparation of the Ketjen Black sulfur composite (KBS). A series of characterization techniques, such as XRD, TEM, XPS, Raman Spectroscopy, and TGA, were employed to validate the synthesis process and investigate the chemical properties of the fabricated materials, which are reported elsewhere.[25]

Electrode formulation and coin cell assembly

The cathodes contain 90 wt.% and 10 wt.% of the composite and polyvinylidene fluoride (PVDF, MTI), respectively. Sulfur loadings were altered by changing the cathode thicknesses. Homogenized cathode slurries were made using NMP (N-methyl-2-pyrrolidone) as the solvent and pasted onto aluminum foil using doctor blades. When the influence of sulfur loading on cell resistance was characterized, we kept the E/S ratio constant (13 mL g^{-1}), and sulfur loadings were adjusted from 0.8 mg cm^{-2} to 3 mg cm^{-2}. Coin cells containing E/S ratios of 6, 13, 20, and 35 mL g^{-1} were constructed with 1.2 mg cm^{-2} sulfur loading to examine the impact of electrolyte quantity on cell resistances.

Two-electrode CR2032 coin cells were fabricated by means of a lithium metal anode (with 170 μm thickness and 2.01 cm^2 area, MTI), the prepared sulfur cathode (with varying thicknesses and an area of 2.01 cm^2), and a Celgard polymeric separator (with 25 μm thickness and 3.1 cm^2 area, MTI). The cells were prepared in an MBraun Labstar glovebox with water and oxygen contents lower than 0.5 ppm. The electrolyte applied here consisted of 1 M lithium bis-trifluoro methanesulfonamide (LiTFSI) and 0.1 M lithium nitrate (LiNO$_3$, both Sigma Aldrich), mixed with 1,2-Dimethoxyethane (DME, Sigma Aldrich) and 1,3-Dioxolane (DOL, Sigma Aldrich) at 1 : 1 volume ratio.

Electrochemical measurements and performance modeling

Electrochemical impedance spectroscopy measurements were conducted at ambient temperature with a Biologic SP300 potentiostat/galvanostat. A 16-hour rest period was given to the cells at open circuit voltage, followed by discharge at 0.1 C rate using a potential range of 1.7 V- 3.0 V. EIS measurements were taken before the first discharge and after the first, tenth, and twentieth discharges of the Li–S cell. The voltage amplitude and frequency range for the EIS studies were set at 10 mV and 10 mHz-100 kHz, respectively. The collected EIS spectra were then fitted with an equivalent circuit model (described in the Results and Discussion section) using Bio-Logic Zfit software. The "Randomize + Simplex" method was utilized with 1000 fitting and randomization iterations. Cyclic voltammetry (CV) measurements were also conducted at room temperature from 2.8 to 1.7 V with a scan rate of 0.1 mV s^{-1}. System-level specific energies were estimated using a modified version of the BatPaC model, initially developed for Li-ion batteries.[38] In the modified version, the system-level design considerations, such as module and utility design, were similar to the original model. Still, a one-dimensional concentration-independent electrochemical model was introduced to describe the current-voltage relationship in the cell. Moreover, the system-level performance model was revised to consider experimental inputs, including specific capacity, S : C : binder wt.%, and material properties.[39,40,41,42] Experimentally tested sulfur loadings and E/S ratios were fed into the model by altering electrolyte vol.% and electrode thickness parameters.

Conflict of Interests

The authors declare no conflict of interest.

Data Availability Statement

The data that support the findings of this study are available from the corresponding author upon reasonable request.

[1] S. Drvaric Talian, J. Moskon, R. Dominko, M. Gaberscek, *Adv. Mater. Interfaces.* **2022**, 9.
[2] J. Conder, C. Villevieille, S. Trabesinger, P. Novak, L. Gubler, R. Bouchet, *Electrochim. Acta.* **2017**, *244*, 61.
[3] M. Rao, X. Song, E. J. Cairns, *J. Power Sources.* **2012**, *205*, 474.
[4] C. McCreary, Y. An, S. U. Kim, Y. Hwa, *Batteries.* **2021**, *7*, 1.
[5] Y. Yuan, Z. Fang, M. Liu, *Int. J. Electrochem. Sci.* **2017**, *12*, 1025.
[6] H. Zhang, X. Qin, J. Wu, Y. B. He, H. Du, B. Li, F. Kang, *J. Mater. Chem. A.* **2015**, *3*, 7112.
[7] J. Shim, K. A. Striebel, E. J. Cairns, *J. Electrochem. Soc.* **2002**, *149*, A1321.
[8] R. Xu, J. C. M. Li, J. Lu, K. Amine, I. Belharouak, *J. Mater. Chem. A.* **2015**, *3*, 4170.
[9] J. Bruckner, S. Thieme, H. T. Grossmann, S. Dorfler, H. Althues, S. Kaskel, *J. Power Sources.* **2014**, *268*, 82.
[10] S. R. Chen, Y. P. Zhai, G. L. Xu, Y. X. Jiang, D. Y. Zhao, J. T. Li, L. Huang, S. G. Sun, *Electrochim. Acta.* **2011**, *56*, 9549.
[11] A. Bhargav, J. He, A. Gupta, A. Manthiram, *Joule.* **2020**, *4*, 285.
[12] S. Urbonaite, T. Poux, P. Novak, *Adv. Energy Mater.* **2015**, *5*, 1.
[13] Y. Ansari, S. Zhang, B. Wen, F. Fan, Y. M. Chiang, *Adv. Energy Mater.* **2019**, *9*, 1.
[14] X. B. Cheng, J. Q. Huang, H. J. Peng, J. Q. Nie, X. Y. Liu, Q. Zhang, F. Wei, *J. Power Sources.* **2014**, *253*, 263.
[15] T. Zerrin, R. Shang, B. Dong, E. C. Aguilar, J. Malvin, M. Ozkan, C. S. Ozkan, *Nano Energy.* **2022**, *104*, 107913.
[16] J. Blair, D. S. Mebane, *Solid State Ionics* **2015**, *270*, 47.
[17] F. Ciucci, *Electrochim. Acta.* **2013**, *87*, 532.
[18] R. Pongilat, S. Franger, K. Nallathamby, *J. Phys. Chem. C.* **2018**, *122*, 5948.
[19] J. Yan, X. Liu, B. Li, *Adv. Sci.* **2016**, *3*, 1600101.
[20] Z. Deng, Z. Zhang, Y. Lai, J. Liu, J. Li, Y. Liu, *J. Electrochem. Soc.* **2013**, *160*, A553.
[21] W. Wang, Y. Wang, Y. Huang, C. Huang, Z. Yu, H. Zhang, A. Wang, K. Yuan, *J. Appl. Electrochem.* **2010**, *40*, 321.
[22] J. Fang, W. Shen, S. H. S. Cheng, S. Ghashghaie, H. K. Shahzad, C. Y. Chung, *J. Power Sources.* **2019**, *441*, 227202.
[23] M. J. Lacey, *ChemElectroChem* **2017**, *4*, 1997.
[24] K. Sun, H. Liu, H. Gan, *J. Electrochem. Energy Convers. Storage.* **2016**, *13*, 1.
[25] A. Kilic, D. Eroglu, *ChemElectroChem.* **2021**, *8*, 963.
[26] H. Fazal, D. Eroglu, A. Kilic, B. Dong, N. Ali, J. Zai, X. Qian, *ACS Appl. Energ. Mater.* **2023**, *6*, 6721–6731.

[27] P. A. Nelson, S. Ahmed, K. G. Gallagher, D. W. Dees, *Electrochim. Acta* **2016**, *202*, 131.

[28] C. Yan, W. Li, X. Liu, M. Chen, X. Liu, X. Li, J. Zai, X. Qian, *ACS Appl. Mater. Interfaces.* **2021**, *13*, 48872.

[29] S. Drvaric Talian, J. Moskon, R. Dominko, M. Gaberscek, *ACS Appl. Mater. Interfaces.* **2017**, *9*, 29760.

[30] C. Weller, J. Pampel, S. Dorfler, H. Althues, S. Kaskel, *Energy Technol.* **2019**, *7*.

[31] J. Zheng, D. Lv, M. Gu, C. Wang, J.-G. Zhang, J. Liu, J. Xiao, *J. Electrochem. Soc.* **2013**, *160*, A2288.

[32] M. Zhang, C. Yu, C. Zhao, X. Song, X. Han, S. Liu, C. Hao, J. Qiu, *Energy Storage Mater.* **2016**, *5*, 223.

[33] K. Sun, H. Liu, H. Gan, *J. Electrochem. Energy Convers. Storage.* **2016**, *13*, 021002.

[34] L. A. Middlemiss, A. J. R. Rennie, R. Sayers, A. R. West, *Energy Rep.* **2020**, *6*, 232.

[35] S. Dorfler, S. Walus, J. Locke, A. Fotouhi, D. J. Auger, N. Shateri, T. Abendroth, P. Hartel, H. Althues, S. Kaskel, *Energy Technol.* **2021**, *9*, 2000694.

[36] K. Zhu, C. Wang, Z. Chi, F. Ke, Y. Yang, A. Wang, W. Wang, L. Miao, *Front. Energy Res.* **2019**, *7*.

[37] D. Eroglu, K. R. Zavadil, K. G. Gallagher, *J. Electrochem. Soc.* **2015**, *162*, A982.

[38] A. Nelson, S. Ahmed, K. G. Gallagher, D. W. Dees, 3rd edition; Argonne National Laboratory: Argonne, IL **2019**.

[39] H. M. Bilal, D. Eroglu, *Int. J. Energy Res.* **2022**, *46*, 15926.

[40] H. M. Bilal, D. Eroglu, *J. Electrochem. Soc.* **2021**, *168*, 030502.

[41] N. B. Emerce, D. Eroglu, *J. Electrochem. Soc.* **2019**, *166*, A1490.

[42] A. Kilic, R. Yildirim, D. Eroglu, *Int. J. Energy Res.* **2022**, *46*, 21716.

RESEARCH ARTICLE

In this study, the effect of cathode material on the lithium-sulfur cell resistance is investigated by preparing two different cathodes: by encapsulating sulfur with pure Ketjen black (KBS) and with atomic vanadium and cobalt-modified Ketjen black (VCKBS). Moreover, the influence of key design parameters, namely electrolyte-to-sulfur ratio and sulfur loading, on the cell resistances and battery performance is also compared.
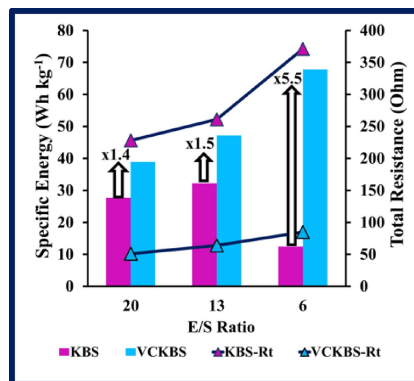
Dr. H. Fazal, Prof. Dr. D. Eroglu*, A. Kilic, Dr. N. Ali, C. Yan, Prof. Dr. J. Zai, Prof. Dr. X. Qian*

1 – 10

Electrochemical Impedance Spectroscopy of Li-S Batteries: Effect of Atomic Vanadium- and Cobalt-Modified Ketjen Black-Sulfur Cathode, Sulfur Loading, and Electrolyte-to-Sulfur Ratio